Role of Functional Groups in Strengthening Polymer−Polymer Interfaces: Random Copolymers with Hydrogen-Bonding Functionalities

Brian D. Edgecombe and Jean M. J. Fréchet*,†

Department of Chemistry, Baker Laboratory, Cornell University, Ithaca, New York 14853-1301, and Department of Chemistry, University of California, Berkeley, California 947290-1460

Zhihua Xu and Edward J. Kramer*,‡

Department of Materials Science and Engineering and the Materials Science Center, Cornell University, Ithaca, New York 14853-1301

Received June 16, 1997. Revised Manuscript Received February 6, 1998

Two series of random copolymers, poly(styrene-d_8-*co*-4-vinylbenzamide) and poly(styrene-d_8-*co*-4-vinyl-*N*-ethylbenzamide), were prepared with varying compositions. The functionalized random copolymers were tested for their abilities to reinforce the weak interface between immiscible polymers: polystyrene and poly(2-vinylpyridine). The effect of the hydrogen-bonding groups with different interaction strengths (primary or secondary benzamide) was studied through the evaluation of interfacial fracture toughness and fracture surface characteristics. For the compositions investigated, the copolymers with the primary benzamide functionality were shown to attain higher fracture toughness values than the substituted benzamide copolymers. Additionally, the composition at which maximum interfacial strengthening was attained was much lower in the primary benzamide case ($f_{max} = 0.06$) than in the substituted benzamide case ($f_{max} = 0.25$). However, in both cases the observed strengthening was lower than our previous results using copolymers bearing phenolic groups. The effect of the copolymer functionality, including such variables as steric constraints and degree of self-association, and composition drift on the measured interfacial properties are discussed.

Introduction

The use of copolymers in enhancing the characteristics of phase domain boundaries in polymer blends has been an appealing strategy for the design of improved polymeric materials. Since the mechanical properties of poorly miscible blends depend strongly on the interfacial strength between polymer phases, copolymers that strengthen the interface also improve the overall material properties. In general the strategy relies on two aspects: (i) a reduction of interfacial energy resulting in larger interfacial widths and (ii) a mechanical connection across the interface capable of transfer of a load. Copolymers of the appropriate length and chemical structure can entangle with the immiscible polymers near the interface and bear the load between phases while also reducing the interfacial energy. Understanding the role of the reinforcing copolymer at the phase boundary between polymers should aid in the design of appropriate copolymers for applications in polymeric composites and adhesives.

Work on the strengthening of interfaces between immiscible glassy polymers, A and B with A−B diblock copolymers has been extensively carried out on model systems such as and polystyrene/poly(methyl methacrylate)[1] and polystyrene/poly(2-vinylpyridine).[2] These studies have yielded some necessary conditions for the effectiveness of a block copolymer in interfacial strengthening: (i) each block of the copolymers must be long enough to entangle effectively with the corresponding homopolymer and (ii) the areal chain density of the copolymer at the phase boundary must be sufficiently large. However, meeting such conditions can cause some practical difficulties. For example, long diblock copolymers tend to form lamellae or other microphase-separated structures. As a result, when increasing amounts of the diblock copolymer are placed at the interface, the strengthening ability of the copolymer reaches a maximum beyond which the interfacial strength actually decreases to a saturation level.

An alternative approach that circumvents this problem involves the use of A−B random copolymers that are prepared through simpler synthetic procedures compared to the conventional preparation of block copolymers via living anionic polymerization. Unexpectedly high fracture toughness values of interfaces have been attained by incorporating significantly lower

* To whom correspondence should be addressed.
† Current address: Department of Chemistry, UC Berkeley, Berkeley, CA, 94720-1460.
‡ Current address: Department of Materials, UC Santa Barbara, Santa Barbara, CA 93106.

(1) Brown, H. R.; Deline, V. R.; Green, P. F. *Nature* **1989**, *341*, 221.
(2) Creton, C. F.; Kramer, E. J.; Hui, C.-Y.; Brown, H. R. *Macromolecules* **1992**, *25*, 3075.

S0897-4756(97)00432-8 CCC: $15.00
Published on Web 03/24/1998

areal chain densities of random copolymers relative to that of block copolymers.[3−8] Recently, Dai et al.[3,4] have proposed a mechanism for the interfacial reinforcement by random copolymers that is consistent with current theories.[9−12] The strengthening is attributed to (i) a high degree of entanglement between random copolymers and polymer A, polymer B, and other random copolymers and (ii) the presence of a composition distribution in the copolymer samples. This composition drift is an artifact of the copolymer synthesis and exists in some random copolymers prepared in high conversion. As a result the copolymer chains segregate in a manner such that A-rich and B-rich copolymers reside along the homopolymer A/copolymer and the homopolymer B/copolymer interfaces, respectively. Through the entanglement of these enriched copolymer chains with the homopolymers and the extensive entanglement within the copolymer layer, a strongly reinforced interface is afforded. Therefore, the multiple points of reinforcements per chain (i.e., entanglements) result in significant strengthening at low areal chain densities.[3,4]

For the A−B copolymers, the only type of interfacial anchoring is the mechanical entanglement of the copolymer on both sides of the interface. However, through the placement of the appropriate functionalities along the copolymer chain, additional sites capable of interfacial interactions can be introduced. For example, Guo et al.[8] have reported the effective reinforcement of a PS/PMMA interface with poly(styrene-*co*-4-vinylpyridine) which was attributed to the formation of a P4VP−PMMA complex. Other interactions such as hydrogen bonding have also been applied to the strengthening of polymer interfaces.

Recently, a random copolymer bearing hydrogen bonding donors, poly(styrene-*co*-4-hydroxystyrene), was used to strengthen the interface between immiscible polymers, polystyrene, and poly(2-vinylpyridine).[13] For this system a drastic increase in the interfacial fracture toughness was observed when copolymers containing less than 5 mol % of 4-hydroxystyrene were used. The pronounced maximum in fracture toughness within the 1−5 mol % range emphasizes the sensitivity of the interface to small changes in the copolymer's degree of functionalization. To further probe the relationship between the functional group and the strengthening ability of a random copolymer, we have extended our study to another family of copolymers with different hydrogen-bonding abilities. Our objective is to gain further understanding of the factors that control interfacial properties through simple variation of the type and extent of functionalization. Specifically, in this study we explore the interfacial strengthening effect of two series of random copolymers bearing amide groups with different N-substitution. Deuterium-labeled copolymers, poly(styrene-d_8-*co*-4-vinylbenzamide) and poly(styrene-d_8-*co*-4-vinyl-*N*-ethylbenzamide), were prepared in order to facilitate the interfacial fracture studies at the polystyrene/poly(2-vinylpyridine) phase boundary as described below in detail.

Experimental Section

Materials. Polystyrene (PS, $M_w = 280\,000$, $M_w/M_n = 2.1$) and poly(2-vinylpyridine), (PVP, $M_w = 200\,000$, $M_w/M_n = 2.4$) were purchased from Aldrich and Polysciences, respectively. Both homopolymers were used as received. Styrene-d_8 was obtained from Cambridge Isotopes Laboratories and simply distilled prior to use in the polymerizations. 4-Vinylbenzoic acid was obtained from Hokko Chemical Industry Co. and used as received. Dicumyl peroxide (DPO) and benzoyl peroxide (BPO) were purified by recrystallization from 95% ethanol and diethyl ether, respectively. Solvents were used as received unless otherwise indicated. All reactions were performed under a steady purge of nitrogen unless otherwise specified.

Methods. Molecular weights of the polymers were determined by SEC on a liquid chromatograph equipped with a differential refractometer (RefractoMonitor, Milton Roy). Tetrahydrofuran (THF) at 40 °C was used as the mobile phase at a nominal flow rate of 1 mL/min. Four 5 μm PL Gel columns with porosities of 100 Å, 500 Å, 1000 Å, and Mixed C were used to achieve separations. The system was calibrated with 20 monodisperse polystyrene standards. Samples that were not soluble in THF were characterized by SEC using *N*,*N*′-dimethylacetamide (DMAC) at 40 °C as the mobile phase. In this case, the liquid chromatograph was equipped with a UV detector ($\lambda = 254$ nm). Calibration was carried out using 15 polystyrene standards. Infrared spectra were recorded on a Nicolet IR/44 spectrophotometer using a suspension of the copolymers in a film of potassium bromide. NMR spectra were recorded on a Bruker AF300 (300 MHz) spectrometer using the solvent proton signal as internal standard. Glass transition temperatures were measured using a Seiko DSC 220C differential scanning calorimeter and a Seiko SSC/5200 thermal analysis station. Heating rates were 20 K/min after an initial annealing run. The glass transition temperature was recorded as the midpoint of the inflection tangent.

4-Vinylbenzoyl Chloride. 4-Vinylbenzoic acid (13.08 g, 0.0882 mol) and 4-*tert*-butylcatechol (10 mg) were added to freshly distilled thionyl chloride (26.21 g, 0.220 mol) at 0 °C under a nitrogen purge. The solution was stirred at 0 °C for 2 h and at room temperature for another 6 h. The solution was then refluxed with a water condenser for 1 h at 40 °C. The excess thionyl chloride was removed via distillation. The acid chloride was isolated via fractional distillation (bp 55 °C, 0.1 mmHg), yield 13.51 g (90% with respect to acid).

4-Vinylbenzamide (1). Freshly distilled 4-vinylbenzoyl chloride (13.40 g, 0.0804 mol, 1.0 equiv) in dry dichloromethane (20 mL) and triethylamine (14 mL) was cooled to 0 °C. Hexamethyldisilazane (31.47 g, 2.4 equiv) in dichloromethane (50 mL) was added slowly to the acid chloride solution via addition funnel. The solution was warmed to room temperature, and the reaction continued for 12 h. After cooling the solution again in an ice bath, the reaction was quenched by slowly adding methanol and then stirring for 2 h at room temperature. The solvent was removed via evaporation, and the product recrystallized from hot 95% ethanol: yield: 9.06 g (76%); ^{1}H NMR (DMSO-d_6) δ 7.97 (br, 1H, NH_2), 7.85 (d, J = 8 Hz, 2H, Ar*H*), 7.54 (d, J = 8 Hz, 2H, Ar*H*), 7.36 (br, 1H, NH_2), 6.88 (2d, J = 11 Hz, 1H, C=C*H*R), 5.93 (d, J = 17 Hz,

(3) Brown, H. R.; Char, K.; Deline, V. R.; Green, P. F. *Macromolecules* **1993**, *26*, 4155.
(4) Dai, C. A.; Dair, B. J.; Dai, K. H.; Ober, C. K. Kramer, E. J.; Hui, C.-Y.; Jelinski, L. W. *Phys. Rev. Lett.* **1994**, *73*, 2472.
(5) Dai, C.-A.; Osuji, C. O.; Jandt, K. D.; Dair, B. J.; Ober, C. K.; Kramer, E. J.; Hui, C.-Y. *Macromolecules* **1997**, *30*, 6727.
(6) Kulasekere, R.; Kaiser, H.; Ankner, J. F.; Russell, T. P.; Brown, H. R.; Hawker, C. J.; Mayes, A. M. *Macromolecules* **1996**, *29*, 5493.
(7) Sikka, M.; Pellegrini, N. N.; Schmitt, E. A.; Winey, K. I. *Macromolecules* **1997**, *30*, 445.
(8) Guo, L.; Rafailovich, M. H.; Sokolov, J.; Peiffer, D.; Schwarz, S. A.; Eisenberg, A. *Bull. Am. Phys. Soc.* **1996**, *41*, 318.
(9) Milner, S. T.; Frederickson, G. H. *Macromolecules* **1995**, *28*, 1357. Milner, S. T.; Frederickson, G. H. *Macromolecules* **1995**, *28*, 7953
(10) Gehlsen, M. D.; Rosedale, J. H.; Bates, F. S.; Wignall, G. D.; Hansen, L.; Almdal, K. *Phys. Rev. Lett.* **1992**, *68*, 2452.
(11) ten Brinke, G.; Karasz, F. E.; MacKnight, W. J. *Macromolecules* **1983**, *16*, 1827. Paul, D. R.; Barlow, J. W. *Polymer* **1984**, *25*, 487.
(12) Kambour, R. P.; Bendler, J. T.; Bopp, R. C. *Macromolecules* **1983**, *16*, 753.
(13) Xu, Z.; Kramer, E. J.; Edgecombe, B. D.; Fréchet, J. M. J. *Macromolecules* **1997**, *30*, 7958.

Table 1. Preparation of Styrene/Vinylbenzamide Random Copolymers

copolymer	type	f [a]	$M_w \times 10^{-5}$	M_w/M_n	initiator/temp (°C)	solvent	% conv
3a	4-vinylbenzamide	0.016	2.06 [b]	2.0	BPO/70	bulk	64
3b		0.032	1.12[b]	1.7	BPO/70	THF	70
3c		0.063	1.74[c]	2.1	BPO/70	THF	43
3d		0.069	3.30[c]	2.5	BPO/70	THF	69
3e		0.250	2.20[c]	2.4	DPO/105	chlorobenzene	63
4a	4-vinyl-*N*-ethylbenzamide	0.065	5.75[b]	2.1	DPO/105	bulk	93
4b		0.113	5.90[b]	2.4	DPO/105	bulk	82
4c		0.195	9.23[c]	2.3	DPO/105	bulk	82
4d		0.240	11.0[c]	2.2	DPO/105	bulk	85
4e		0.455	10.4[c]	1.7	DPO/105	bulk	87

[a] Molar fraction of benzamide monomer in copolymer, determined via elemental analysis and FRES. [b] Molecular weight from SEC in THF using a polystyrene calibration. [c] Molecular weight from SEC in DMAC using a polystyrene calibration.

1H, C═C(H)*H′*), 5.37 (d, J = 11 Hz, 1H, C═C(*H*)H′). Anal. Calcd for C_9H_9NO: C, 73.45; H, 6.16; N, 9.52. Found: C, 73.18; H, 6.18; N, 9.52.

4-Vinyl-*N*-ethylbenzamide (2). A suspension of 4-vinylbenzoyl chloride (8.0 g, 0.048 mol, 1.0 equiv) and $EtNH_2$·HCl (3.95 g, 1.05 equiv) in dichloromethane (80 mL) was prepared in a three-neck round-bottom flask equipped with a dry ice/acetone coldfinger condenser and an addition funnel charged with triethylamine (5.0 equiv). Upon the dropwise addition of the triethylamine to the stirred solution, condensation of liberated ethylamine was observed on the coldfinger. After complete addition (15 min) much precipitate had formed, and the solution was stirred for 2 h. The solution was poured onto 500 mL water and extracted with dichloromethane (3×). The organic layers were combined and washed with dilute aqueous HCl, water, aqueous $NaHCO_3$, and saturated aqueous NaCl. The organic layer was dried over magnesium sulfate, filtered, evaporated to dryness, and recrystallized from EtOAc:hexanes (1:4 v/v) to yield white plates, yield 5.70 g (68%). ^{1}H NMR ($CDCl_3$) δ 7.71 (d, J = 8 Hz, 2H, Ar*H*), 7.43 (d, J = 8 Hz, 2H, Ar*H*), 6.72 (2d, J = 11 Hz, 1H, C═C*H*Ar), 6.18 (br s, 1H, NH), 5.81 (d, J = 17 Hz, 1H, C═C(H)*H′*), 5.33 (d, J = 11 Hz, 1H, C═C(*H*)H′), 3.48 (m, J = 7 Hz, 2H, NH−C*H*$_2$−CH$_3$), 1.24 (t, J = 7 Hz, 2H, NH−CH$_2$−C*H*$_3$). Anal. Calcd for $C_{11}H_{13}NO$: C, 75.40; H, 7.48, N, 7.99. Found: C, 75.13; H, 7.40; N, 8.07.

Preparation of Poly(styrene-d_8-*co*-4-vinylbenzamide) (3a−d). In a typical polymerization styrene-d_8 (2.0 g) and **1** (0.190 g) were combined with benzoyl peroxide (10 mg) with 2 mL of THF. The solution was stirred under nitrogen for 30 min before being placed in a heating bath at 75 °C. The polymerization was carried out under nitrogen and stopped after 20 h. The resulting random copolymer was dissolved in DMF and precipitated into excess 2-propanol/hexane (1:1 v/v). For copolymers with high benzamide content (>15 mol %), the polymerization conditions were altered to accommodate the limited solubility of **1** in styrene-d_8/THF. In this case, the monomers were combined with chlorobenzene in the presence of dicumyl peroxide and heated to 105 °C. The polymers obtained as white powders were filtered and dried in a vacuum oven at 50 °C. Conversions were between 43 and 70%. ^{1}H NMR (DMF-d_7) δ 8.1 (br, Ar*H*), 7.3 (br, Ar*H*), 6.8 (br, Ar*H*), 2.0 (br, −CH$_2$−C(*H*)Ar), 1.5 (br, −C*H*$_2$−C(H)Ar). The compositions of the random copolymers were determined from elemental analysis of copolymer for nitrogen content (Table 1).

Preparation of Poly(styrene-d_8-*co*-4-vinyl-*N*-ethylbenzamide) (4a−e). In a typical polymerization styrene-d_8 (2.0 g) and **2** (0.172 g) were combined with dicumyl peroxide (10 mg). The solution was stirred under nitrogen for 30 min before being placed in a heating bath at 105 °C. The polymerization was carried out in the bulk under nitrogen and stopped after 20 h. The resulting random copolymer was dissolved in THF and precipitated into excess methanol. For copolymers with high benzamide content (>30 mol %), a pyridine solution of the copolymer was prepared and precipitated into 2-propanol/hexane (1:1 v/v). The polymers obtained as white powders were filtered and dried in a vacuum oven at 50 °C. Conversions were between 82 and 93%. ^{1}H NMR (DMF-d_7) δ 8.4 (br, N*H*), 7.8 (br, Ar*H*), 7.2 (br, Ar*H*), 6.7 (br, Ar*H*), 3.5 (br, −C(O)-NH−C*H*$_2$CH$_3$), 1.9 (br, −CH$_2$−C(*H*)Ar), 1.6 (br, −C*H*$_2$−C(H)-Ar), 1.2 (br, NH−CH$_2$C*H*$_3$). The compositions of the random copolymers were determined from elemental analysis of copolymer for nitrogen content (Table 1).

Preparation of Fracture Toughness Samples. For the preparation of the fracture toughness samples, PS and PVP plates were made by compression molding against smooth ferrotype plates. (Such plates can be purchased from photography supply stores.) The PS plate (2.3 mm) was made thicker than the PVP plate (1.7 mm) for reasons described below. A film of the random copolymer was spun-cast from toluene or propyl acetate onto the smooth surface of the PVP plate. For copolymer **3d**, which exhibited poor solubility in most solvents, pyridine was used as the spin-casting solvent. The residual solvent was removed by heating the coated plate in a vacuum oven at 80 °C for 2 h. This plate was then welded to a PS plate at 160 °C for 2 h to form a layered assembly of PS/random copolymer/PVP. This annealing step promotes the diffusion of the random copolymer into the respective homopolymers to form chain entanglements. The sample was then cut with a diamond saw into strips for the subsequent fracture toughness measurements. The dimensions of the strips were 50 mm long × 8.7 mm wide × 4.0 mm thick.

Fracture Toughness Measurements. The fracture toughness of the phase boundary, G_C, which is defined as the critical energy release rate of an interfacial crack, was measured using the asymmetric double-cantilever beam method (ADCB). The measurement was performed at room temperature by inserting a single-edge razor blade at the phase boundary and pushing it at a constant rate of 3×10^{-6} m/s using a servocontrolled motor drive. The steady-state value of the crack length, a, along the phase boundary ahead of the razor blade was measured at regular time intervals. Using these values of a, the fracture toughness G_C, which is proportional to a^{-4}, was computed.[2] The error bars reported subsequently for G_C represent standard deviation of at least 16 measurements of the crack length. More details about the ADCB fracture test can be found elsewhere.[2,14] As shown by Xiao et al.,[14] the effect of shear stresses developing ahead of the crack on the measured toughness is minimized at the mechanical phase angle $\psi \approx -6$. Therefore, interfacial fracture toughness measurements were carried out using PS and PVP plates with thicknesses of 2.3 and 1.7 mm, respectively, which produce this mechanical phase angle, ψ.

The use of deuterium-labeled copolymers in this study allowed for the determination of the role of the copolymer in the failure mechanism. After the fracture toughness measurement, the fracture surfaces of each test specimen were examined with forward recoil spectrometry (FRES)[15] to determine the amounts of deuterium from the residual copolymer. Using these data for each specimen, we calculated the apparent thickness and areal chain density of random copolymer on both PS (t_{PS} and Σ_{PS}, respectively) and PVP (t_{PVP} and Σ_{PVP}, respectively) sides. The total areal chain density, Σ, and

(14) Xiao, F.; Hui, C.-Y.; Washiyama, J.; Kramer, E. J. *Macromolecules* **1994**, *27*, 4382.

(15) Doyle, B. L.; Peercy, P. S. *Appl. Phys. Lett.* **1979**, *34*, 811. Mills, P. J.; Green, P. F.; Palmstrøm, C. J.; Mayer, J. W.; Kramer, E. J. *Appl. Phys. Lett.* **1984**, *45*, 957.

Scheme 1

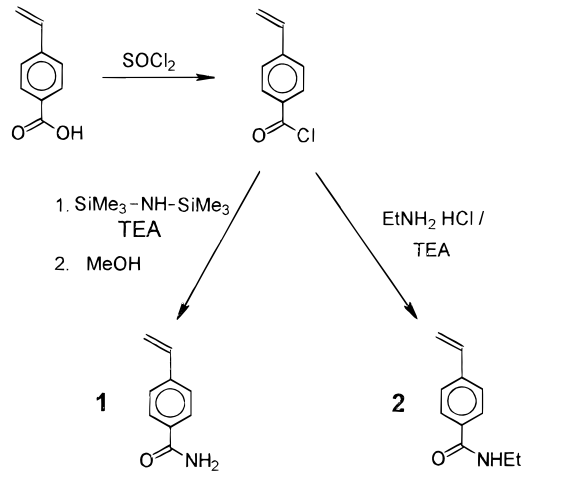

Scheme 2

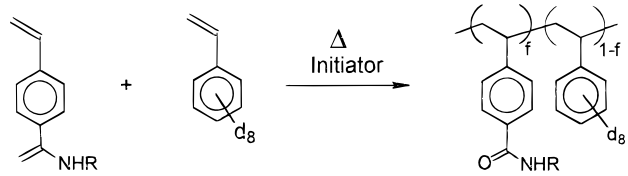

R = H **3(a-e)**
= Et **4(a-e)**

thickness, *t*, of the copolymer was calculated by summing these two measurements; i.e., $\Sigma = \Sigma_{PS} + \Sigma_{PVP}$; $t = t_{PS} + t_{PVP}$.

The fracture study results are compared in the discussion below by plotting both fracture toughness and the fraction of ^2H on the PS side after fracture (Σ_{PS}/Σ) as functions of the amount of copolymer placed at the interface (copolymer layer thickness, *t*, and areal chain density, Σ). The solid line is our qualitative interpretation of the data trend. In the absence of copolymer the fracture toughness of the phase boundary is approximately 2 J/m^2.

Results and Discussion

Preparation of Random Copolymers. Monomers bearing amide functional groups, 4-vinylbenzamide (**1**) and 4-vinyl-*N*-ethylbenzamide (**2**), were synthesized for use in a variety of copolymerizations with styrene-d_8. While 4-vinylbenzamide has been prepared from (2-bromoethyl)benzene by Asahara et al.,[16] no prior report of the preparation of the *N*-ethyl derivative has been found in the literature. In view of the commercial availability of 4-vinylbenzoic acid, this monomer was used to prepare both monomers as shown in Scheme 1. Conversion of 4-vinylbenzoic acid to the corresponding acid chloride was followed by reaction with either hexamethyldisilazane or ethylamine hydrochloride in the presence of triethylamine to afford 4-vinylbenzamide (**1**) and 4-vinyl-*N*-ethylbenzamide (**2**) in 67 and 61% overall yields, respectively.

High molecular weight random copolymers of **1** and of **2** with styrene-d_8 were prepared via solution and bulk radical polymerization (Scheme 2). Conditions were varied depending on monomer feed ratios (Table 1). Because of the poor solubility of the primary benzamide in neat styrene-d_8, the preparation of copolymers **3a**−**d** was carried out in solvent in order to obtain a homogeneous solution. Conversions for the copolymerizations of **1** and styrene-d_8 were moderate (Table 1). Solubility of the copolymers with high benzamide loadings, **3c**,**d**, was limited to polar solvents such as pyridine or DMAC. For this reason, measurement of the molecular weight of copolymers **3c**,**d** was carried out by SEC using DMAC as the mobile phase. Since calibration standards of polymers with a similar molecular structure are not readily available, all relative molecular weights were determined from a polystyrene calibration in DMAC. The specific interactions between DMAC and the benzamide copolymers are expected to introduce some error into the molecular weight determination. Nonetheless, in this study the molecular weight values are useful for comparison among the copolymers within a given series. Copolymers **3a**−**c** exhibit glass transitions temperature between 105 and 140 °C, depending on composition, while for **3d** a glass transition was measured to be 160 °C.

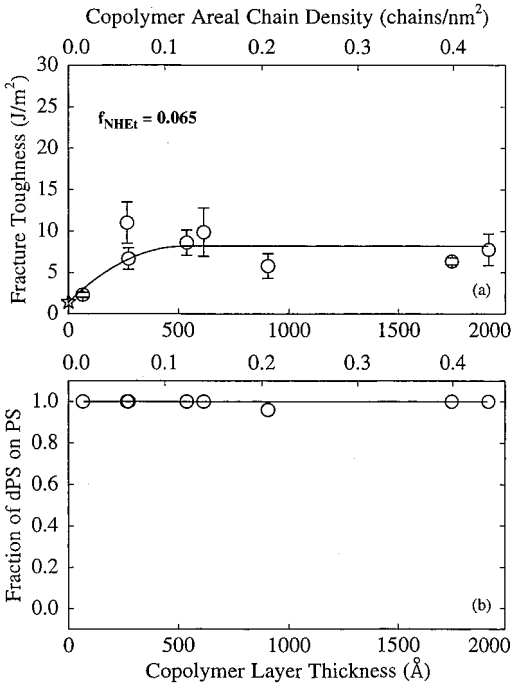

Figure 1. (a) Fracture toughness and (b) fraction of deuterated polystyrene, dPS, units from the copolymer on the polystyrene side of the interface after fracture plotted as a function of **4a** copolymer layer thickness.

Since 4-vinyl-*N*-ethylbenzamide is freely soluble in styrene-d_8 under the polymerization conditions, the preparation of copolymers **4a**−**e** was carried out in the bulk. All of the copolymers exhibited glass transition temperatures between 105 and 140 °C. In general, the solubility characteristics of the *N*-ethylbenzamide copolymers were superior to those of the primary benzamide copolymers. Copolymers **4a**−**d** showed good solubility in dichloromethane, THF, and pyridine, while **4e** was only soluble in polar solvents such as pyridine and DMAC.

Fracture Toughness Measurements. The interfacial fracture toughness plotted against the thickness of the copolymer layer placed at the PS/PVP interface is shown in Figures 1a and 2a for poly(styrene-d_8-*co*-4-vinyl-*N*-ethylbenzamide) samples **4a** and **4e**, respec-

(16) Asahara, T.; Yoda, N. *J. Polym. Sci.: Part A-1* **1968**, *6*, 2477.

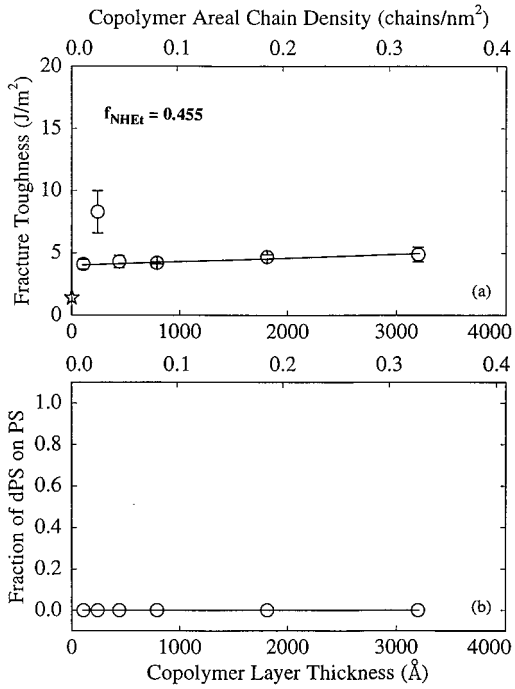

Figure 2. (a) Fracture toughness and (b) fraction of deuterated polystyrene, dPS, units from the copolymer on the polystyrene side of the interface after fracture plotted as a function of **4e** copolymer layer thickness.

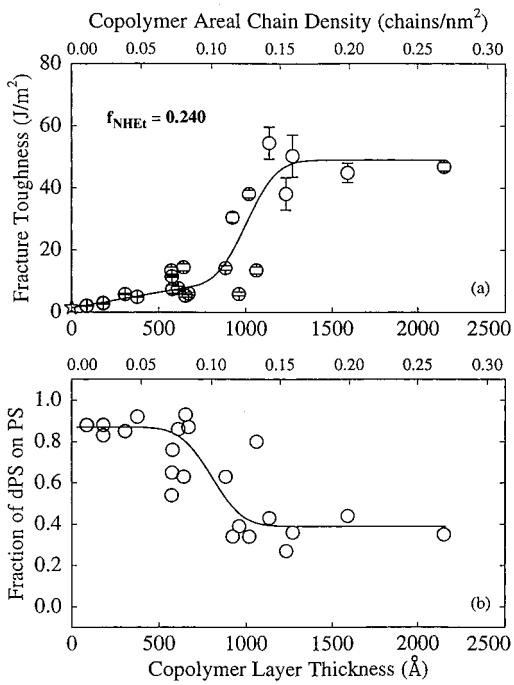

Figure 3. (a) Fracture toughness and (b) fraction of deuterated polystyrene, dPS, units from the copolymer on the polystyrene side of the interface after fracture plotted as a function of **4d** copolymer layer thickness.

tively. In both cases, the interfacial strengthening is low such that craze formation does not occur at any copolymer layer thickness. The reason for the low degree of strengthening afforded by copolymers with these compositions ($f = 0.065$ and $f = 0.455$) is made clear by examining the PS and PVP surfaces after fracture using FRES. In Figures 1b and 2b the fractions of deuterium from the copolymers **4a** and **4e** on the PS surface are plotted as a function of total copolymer layer thickness. Representation of the data in this fashion is helpful in the determination of the locus of crack propagation. The fraction of copolymer remaining on the PS surface after fracture is strikingly different for the two copolymers, **4a** and **4e**. In the case of the copolymer with a higher extent of functionalization, **4e**, the copolymer resides exclusively on the PVP side after fracture except at low thicknesses. In contrast, copolymer **4a** is found only on the PS side. Therefore, if we treat the copolymer as a discrete layer, the crack propagates in the former case along the weak PS/copolymer interface and, in the latter, along the weak PVP/copolymer interface. The weakness of the interfaces reinforced with **4e** is attributed to the poor entanglement between the highly functionalized copolymer and the PS homopolymer which results in failure by chain pull-out. Analogously, the styrene-rich random copolymer, **4a**, does not entangle with the PVP homopolymer and the interface fails by pull-out near the PVP side. In both cases, the poor degree of entanglement is most likely a consequence of the narrow interfacial width resulting from the copolymer/homopolymer immiscibility.

The plot of fracture toughness as a function of copolymer layer thickness for **4d**, a copolymer with an intermediate composition ($f = 0.24$), is shown in Figure 3a. As the amount of copolymer placed at the interface is increased, we initially observe a regime in which only slight strengthening occurs ($t^* < 750$ Å, $\Sigma^* < 0.11$ chain/nm^2), followed by a transition region in which the fracture toughness increases rapidly, and then a saturation regime ($G_C = 50$ J/m^2). This strengthening dependence is qualitatively similar to that seen in other block and random copolymer studies in which a transition occurs in the fracture mechanism from a combination of chain pull-out and chain scission (low Σ) to craze formation (high Σ).[3−5] (A detailed study of the transitions in the fracture mechanism can be found elsewhere.[2,17]) The deduction that both pull-out and chain scission occur during fracture follows from the observed value of the critical areal chain density ($\Sigma^* = 0.11$ chain/nm^2). In earlier studies with long diblock copolymers that undergo one scission per chain during fracture, the chain scission-to-crazing transition is seen at $\Sigma^* = 0.03$ chain/nm^2. Since the transition value is dependent only on the number of scissions per chain and not on the copolymer architecture, a reinforcing copolymer that causes a transition above 0.03 chain/nm^2 must have only a fraction of the chains breaking during fracture. Therefore, in the case of copolymer **4d**, only 27% (0.03/0.11) of the copolymers can be undergoing chain scission.

In Figure 3b it is observed that below the critical areal chain density ($\Sigma^* = 0.11$ chain/nm^2) deuterated styrene units are found predominantly on the PS surface after fracture (90%). This distribution of copolymer is consistent with chain scission occurring along a plane near the PVP. At the critical areal chain density, Σ^*, a sudden change in the deuterium distribution from 90% to 40% on the PS side suggests a change in the locus of fracture to a plane within the copolymer layer. It is noteworthy that this transition in the deuterium distribution is different from that seen in the previous study[13] with poly(styrene-*co*-4-hydroxystyrene) where no

(17) Washiyama, J.; Kramer, E. J.; Hui, C.-Y. *Macromolecules* **1993**, *26*, 2928.

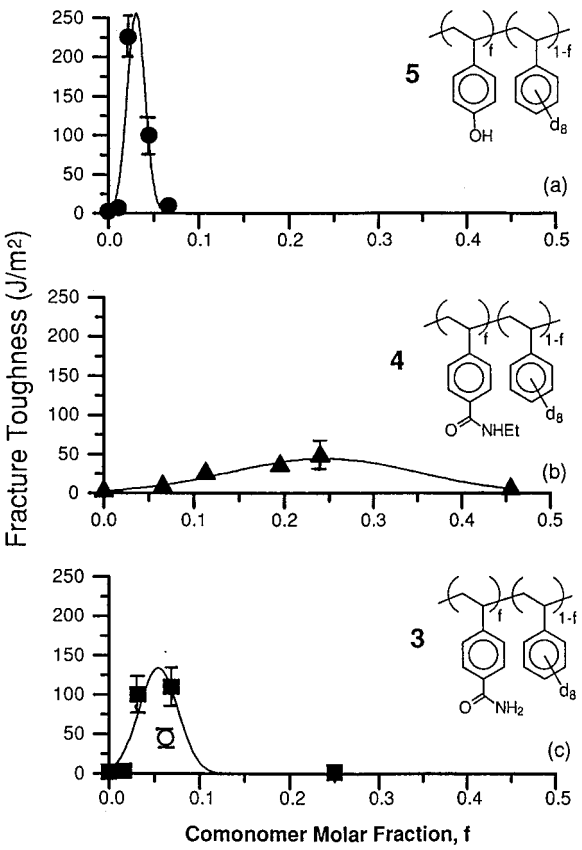

Figure 4. Fracture toughness plotted as a function of comonomer molar fraction, *f*, for copolymer series (a) **5**, (b) **4**, and (c) **3.** Open circle in (c) corresponds to copolymer polymerized to lower conversion. Fracture toughness values are taken from saturation levels and, therefore, are independent of copolymer layer thickness.

copolymer was observed on the PS side after fracture. In that case craze propagation likely occurred within the PS homopolymer near the copolymer/PS interface.

The strengthening behavior and deuterium distribution after fracture of an interface reinforced with **4c** (data not shown) is observed to be very similar to the case with **4d** although a slightly lower toughness (G_C = 40 J/m^2) is attained in the large Σ limit. For interfaces reinforced with **4b**, $f = 0.113$, a scission-to-crazing transition is also observed beyond which G_C = 25. However, the deuterium is found on the PS side after fracture for all areal chain densities indicating the propagation of the crack along the PVP/copolymer interface (data not shown).

The results from the fracture toughness measurements for copolymers **4a**−**e** is replotted in Figure 4b using the fracture toughness at saturation (G_C in the large Σ limit) as a function of copolymer composition, *f*. We compare this plot with data in Figure 4a from a previous study[13] using a random poly(styrene-*co*-4-hydroxystyrene), **5**, as the interfacial strengthening agent. Although in both cases a maximum fracture toughness is obtained at a critical molar fraction of functionalized monomer (f_{max}), several significant differences are apparent.

First, the values of f_{max} are strikingly different in the two studies: f_{max}(**5**) ≈ 0.03 and f_{max}(**4**) ≈ 0.25. In other words, with the *N*-ethylbenzamide functional group a loading almost 1 order of magnitude higher than with the hydroxystyrene group is needed in order to create sufficiently strong interactions between the copolymer and the homopolymers near the interface. Second, the maximum interfacial fracture toughness is much lower in the case of **4** (G_C = 50 J/m^2) than that of **5** (G_C = 220 J/m^2). Therefore, from these observations it appears that the interaction between the substituted benzamide and the pyridyl group is considerably weaker than the phenol−pyridyl interaction when these functionalities are polymer pendant groups. Additionally, the enthalpic penalty of poly(4-vinyl-*N*-ethylbenzamide)−PS interactions is most likely less than that of poly(4-hydroxystyrene)−PS interactions.

Finally, the sensitivity of fracture toughness to copolymer composition is lower in the case of the *N*-ethylbenzamide copolymers, **4a**−**e**. While the strengthening of the hydroxystyrene random copolymers with compositions deviating from f_{max}(**5**) was found to decrease drastically, *N*-ethylbenzamide copolymers with compositions far from the f_{max}(**4**) maintain some reinforcing ability. This difference may in part be caused by the composition drift that may be present in the benzamide copolymers but is not expected in the hydroxystyrene copolymers[13] since in the polymerization of styrene/*t*-BOC-protected hydroxystyrene the reactivity ratios are both equal to 1.[18] The reactivity ratios for **2** and styrene-d_8 were not measured in the context of this study, and the possibility that a significant distribution of copolymer compositions exists in which one specific formulation is strongly interacting cannot be discounted.

Compared to the substituted benzamide copolymers, the copolymers bearing primary benzamide groups show a greater ability to strengthen the PS/PVP interface. In Figure 5a the fracture toughness data for an interface reinforced by **3d** (f = 0.069) is plotted against the copolymer layer thickness. A transition is observed with a high saturation fracture toughness value near 110 J/m^2. Since the copolymer is predominantly on the PVP side after fracture, it appears that for the **3d**-reinforced interface a craze forms and widens into the less craze-resistant homopolymer, PS, with subsequent fibril failure occurring near the PS/copolymer interface. At the lower molar composition of **3b** (f = 0.032), while the interface is significantly strengthened, the deuterium distribution data suggest a change in the locus of fracture as in the case for **4d** (data not shown).

The primary benzamide copolymer of intermediate composition **3c** (f = 0.063), was observed to reinforce the PS/PVP interface to a lesser degree (Figure 6) than **3b** and **3d**. This behavior is unexpected in light of the trends exhibited in fracture toughness as a function of copolymer composition, (Figure 4a,b). However, the sample **3c** was prepared in relatively low conversion (43%) compared to the other copolymers in the series **3a**−**e**. Since copolymer drift is less prevalent in a polymerization of low conversion, the aberration in the strengthening ability of the copolymer **3c** is most likely due to the absence of styrene-rich copolymers. According to the results of the interfacial fracture measurements (not shown), copolymers **3a** (f = 0.016) is found to be too styrene-rich to reinforce the PVP/copolymer

(18) Jongsma, T.; Kimkes, P.; Challa, G. *Polym. Commun.* **1991**, *32*, 34.

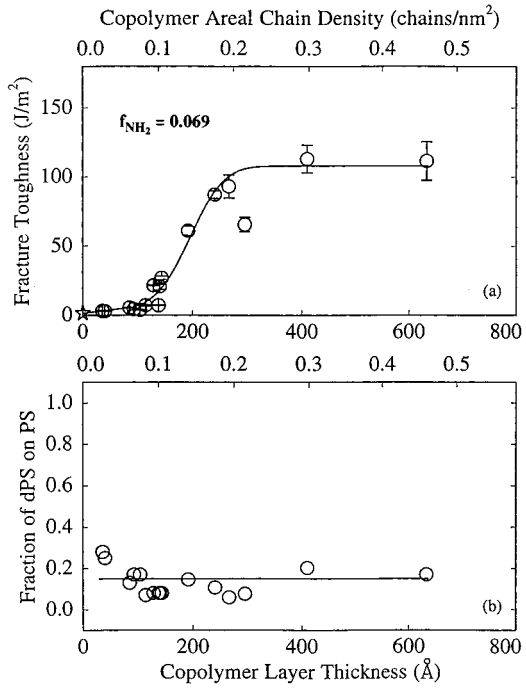

Figure 5. (a) Fracture toughness and (b) fraction of deuterated polystyrene, dPS, units from the copolymer on the polystyrene side of the interface after fracture plotted as a function of **3d** copolymer layer thickness.

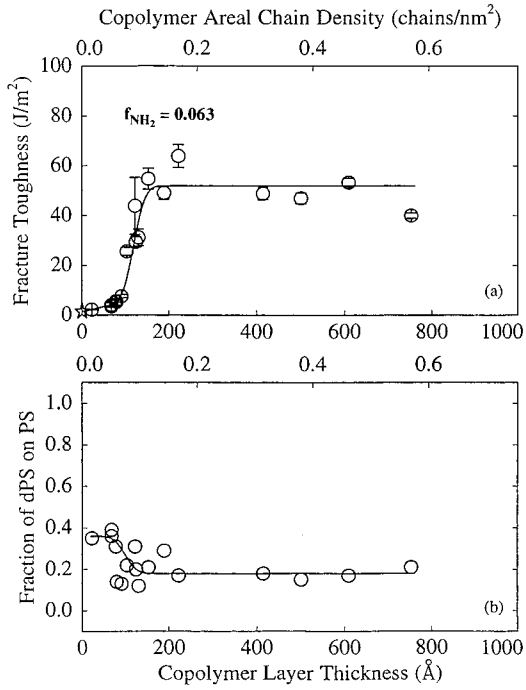

Figure 6. (a) Fracture toughness and (b) fraction of deuterated polystyrene, dPS, units from the copolymer on the polystyrene side of the interface after fracture plotted as a function of **3c** copolymer layer thickness.

interface while **3e** (f = 0.25) is too benzamide-rich to reinforce the PS/copolymer interface. Therefore, in both cases fracture toughness values were below 10 J/m^2. This behavior is consistent with the trends seen for the other random copolymers described above.

Similar to the trend for the substituted benzamide copolymers **4a**−**e**, the plot of fracture toughness at saturation vs copolymer composition for **3a**−**e** in Figure 4c suggests a broader window of copolymer compositions that afford strong interfaces as compared to that seen in the poly(styrene-*co*-4-hydroxystyrene) study. The fracture toughness attained with interfaces reinforced with **3c** is included as an open circle. For the series of primary benzamide copolymers characterized in this study, **3a**−**d**, the highest attainable fracture toughness is still below that found for poly(styrene-*co*-4-hydroxystyrene). The trace in Figure 4c suggests a value of $f_{max} \approx 0.06$ for the primary benzamide copolymers, which is an intermediate value between that of the *N*-ethylbenzamide and the hydroxystyrene copolymers. According to these data, it is possible to tune the interfacial strength within a range of values.

The difference in the effectiveness of the random copolymers in interfacial strengthening may be correlated to the effect of structure on the type and strength of the hydrogen bonds. In general, both self-association and heteroassociation play important roles in determining the overall interaction energy of a hydrogen-bonding system and must be considered in order to understand the observed trends. Studies of hydrogen-bonding interactions between small molecules are readily available from the literature and serve as useful models for analogous polymer−polymer interactions. For example, the ability of amides to interact via hydrogen bonding is known to be very sensitive to their exact chemical structures. Specifically, a comparison of the self-association of benzamide and *N*-methylbenzamide leads to enthalpies of interaction of −9.0 and −3.6 kcal/mol, respectively.[19] The energetic difference has been attributed to an equilibrium strongly in favor of two hydrogen bonds in the case of the primary benzamide, whereas for the substituted benzamide only one hydrogen bond is present on average. In the latter case, the formation of two H-bonds is not favorable as a result of steric crowding from the methyl group. We expect that the copolymers incorporating either 4-vinylbenzamide or 4-vinyl-*N*-ethylbenzamide will also self-associate in a fashion analogous to the small molecule models. Therefore, based upon self-association alone one may expect that the *N*-ethylbenzamide functionality would be more available for interaction with another hydrogen-bond acceptor and more strongly interacting. Of course, the interaction of the *N*-ethylbenzamide copolymers with the poly(2-vinylpyridine) (heteroassociation) is also expected to be greatly hindered by the N-substitution. Unfortunately, no data on the interaction energies between benzamide and pyridine compounds were found in the literature.

Although model compound studies can be helpful, studies of the interaction between the polymer-bound functionalities are more applicable to our strengthening studies. Recent segregation studies[20] of PS−PVP diblock copolymers to a PS/benzamide copolymer interface show a large difference in the interfacial excess of diblock copolymer depending on the substitution of the benzamide copolymer. For example, the interfacial excess of PS−PVP diblock copolymer at a PS/poly(styrene-*co*-4-vinyl-*N*-ethylbenzamide) interface after annealing was

(19) Pimentel, G. C.; McClellan, A. L. *The Hydrogen Bond*; W. H. Freeman and Company: New York, 1974.

(20) Xu, Z.; Kramer, E. J.; Edgecombe, B. D.; Fréchet, J. M. J., unpublished data.

negligible for $f = 0.17$. In contrast, large interfacial excesses were observed for PS/poly(styrene-*co*-4-vinylbenzamide) interface where $f = 0.08$ and $f = 0.21$. In fact, with the primary benzamide interfaces, microemulsion phases were formed as in the case of an earlier segregation study with poly(styrene-*co*-4-hydroxystyrene).[21] In light of the hydrogen-bonding data for small molecules and the segregation study results, it is reasonable that the following trend for interfacial strengthening ability is observed for the functionalized random copolymers: poly(styrene-*co*-4-hydroxystyrene) > poly(styrene-*co*-4-vinylbenzamide) > poly(styrene-*co*-4-vinyl-*N*-ethylbenzamide).

For practical applications of these copolymers as strengthening agents, it would be useful to quantify the interaction between poly(4-vinylbenzamide), PS(Am), mer units and the PS and PVP mer units in order to predict the interfacial characteristics of copolymers with different compositions. If we treat the random copolymer as a distinct, separate phase, the Flory−Huggins interaction parameter, χ, based on the mer units can be obtained in a straightforward manner by using data from our strengthening results and recent segregation studies. In this treatment three interaction parameters are involved ($\chi_{PS(Am)-PS}$, χ_{PS-PVP}, and $\chi_{PS(Am)-PVP}$) which give rise to the effective Flory−Huggins interaction parameters between the random copolymer (rcp) and PS:[11]

$$\chi_{rcp-PS} = f^2 \chi_{PS(Am)-PS} \quad (1)$$

and between the random copolymer and PVP:

$$\chi_{rcp-PVP} = (1 - f)\chi_{PS-PVP} + f\chi_{PS(Am)-PVP} - f(1 - f)\chi_{PS(Am)-PS} \quad (2)$$

From segregation studies described above, the effective interaction parameter of a random copolymer with $f = 0.08$ was determined to be χ_{rcp-PS} ($f = 0.08$) = 0.03.[20] This condition sets an approximate lower limit for $\chi_{PS-PS(Am)} \approx 4.6$ according to eq 1.

In the large Σ limit the primary benzamide random copolymer/PS interface becomes strong enough to support a craze only below $f \approx 0.10$ as seen in Figure 4c. Therefore, below this composition, the $\chi_{rcp-PVP}$ should be comparable in magnitude to the interaction parameter that was determined for a relatively weak PS−PVP random copolymer/PS interface, $\chi_{rcp-PS} \approx 0.015$.[5] Using eq 2, we can estimate the value of $\chi_{PS(Am)-PVP}$ which satisfies the condition that $\chi_{rcp-PVP} < 0.015$ at $f = 0.1$. Using values of $\chi_{PS-PVP} \approx 0.12$ (ref 22) and $\chi_{PS-PS(AM)} \approx 4.7$, the calculation affords a value of $\chi_{PS(Am)-PVP} \approx 3.3$. Although this analysis does not take into account the possibility of composition drift in the random copolymers, it is useful for the estimation of the interaction parameters.

Interestingly, the analysis suggests that the large, positive $\chi_{PS-PS(Am)}$ is responsible for the strong random copolymer/PVP interface via the well-known copolymer effect.[9,11] This general effect was originally described for the miscibility of polymer/random copolymer mixtures in which a "repulsion" between covalently linked comonomers was primarily responsible for inducing miscibility in the system. In other words, the presence of attractive interactions is not required for a polymer/copolymer system to be miscible. Clearly, from the value of $\chi_{PS(Am)-PVP} \approx 3.3$ an attractive interaction does not exist between the random copolymer and the PVP phase. Nonetheless, since the enthalpic penalty of the PS(Am)−PVP contacts is less than that of the PS(Am)−PS contacts, the copolymer interacts with the PVP to a sufficient extent to reinforce the interface. Therefore, the copolymer effect plays an important role in the interpretation of the interactions of the copolymer at the interfaces. The origin of the large interaction parameters is attributed to the strong self-association of benzamides via hydrogen bonding. The limited ability of the benzamide to interact with the poly(2-vinylpyridine) moieties and compensate for the self-association is most likely due to the steric hindrance of the pyridyl group substituted in the 2-position.

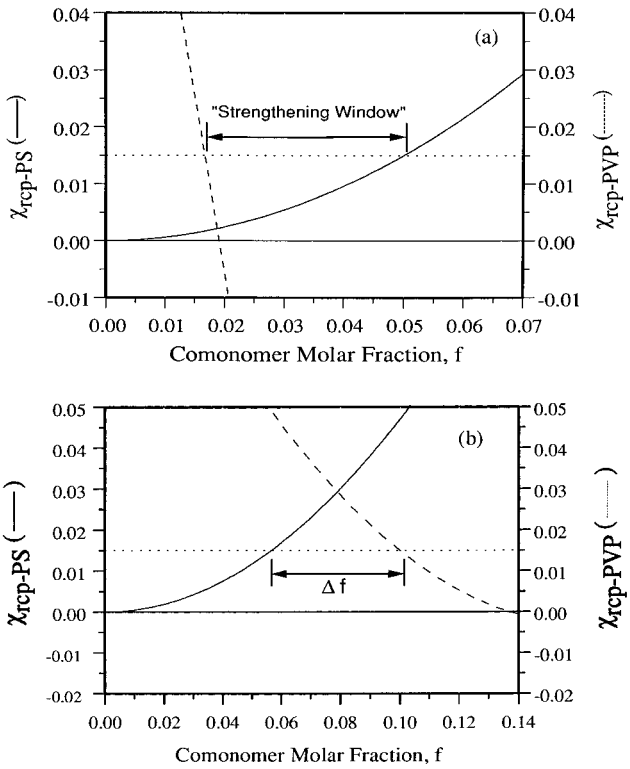

Figure 7. Effective interaction parameters, χ_{rcp-PS} and $\chi_{rcp-PVP}$, as functions of copolymer composition, *f*, for (a) poly(styrene-d_8-*co*-4-hydroxystyrene) and (b) poly(styrene-d_8-*co*-4-vinylbenzamide), where *f* is the molar fraction of 4-hydroxystyrene and 4-vinylbenzamide, respectively. $\chi_{eff} = 0.015$ (dotted line) is the maximum value for which a strong rcp/homopolymer interface is formed.

To predict the copolymer composition range that affords strong interfaces, it is useful to simultaneously plot the effective interaction parameters, χ_{rcp-PS} and $\chi_{rcp-PVP}$, as functions of composition from eqs 1 and 2. In Figure 7 the effective interaction parameters are plotted for both hydroxystyrene copolymers and primary benzamide copolymers using $\chi_{PS(OH)-PS} \approx 6.0$,[13] $\chi_{PS(OH)-PVP} \approx -0.28$,[23] $\chi_{PS(Am)-PS} \approx 4.6$, and $\chi_{PS(Am)-PVP} \approx 3.3$. Additionally the condition that the effective interaction parameter must be less than 0.015 for a strong interface

(21) Xu, Z.; Jandt, K. D.; Kramer, E. J.; Edgecombe, B. D.; Fréchet, J. M. J. *J. Polym Sci.: Part B: Polym. Phys.* **1995**, *33*, 2351. Xu, Zhihua, Ph.D. Thesis, Cornell University, 1997, available from University Microfilms.

(22) Dai, K. H.; Kramer, E. J. *Polymer* **1993**, *35*, 157.

is introduced as a dotted line. Therefore, only the portion of the curves below the value of 0.015 corresponds to compositions that afford a strong PS/rcp or PVP/rcp interface. For the composition regime where both curves are below 0.015, both interfaces are strong and the measured toughness should be high. In case of PS−PS(OH) random copolymers a strengthening "window" is expected for $0.018 < f < 0.050$ (Figure 7a). This prediction corresponds well with Figure 4a.

However, the model for the primary benzamide copolymers predicts that no composition exists for which both PS/rcp and PVP/interfaces are strong. In other words, at $\chi_{eff} = 0.015$, a gap, $\Delta f = 0.043$, is observed between the highest composition that affords a strong PS/rcp interface and the lowest composition that affords a strong PVP/rcp interface. Therefore, the most probable explanation for our observation shown in Figure 4b is a distribution of compositions in our copolymer samples such that some copolymer chains have $f < 0.057$ and some $f > 0.10$. If such a distribution of compositions existed in our samples, a high interfacial fracture toughness would be observed.

Conclusion

This study confirms the importance of polymer−polymer interactions such as hydrogen bonding[24] in assembling systems constituted of dissimilar components. By preparing random copolymers bearing different functional groups, the relationship between copolymer functionality and interfacial reinforcement was investigated. While poly(styrene-*co*-2-vinylpyridine) can strengthen the PS/PVP interface at 50:50 composition through nonspecific interactions, copolymers capable of hydrogen-bonding interactions exhibit a range of strengthening at low-to-moderate loading of functional groups. The specific characteristics of the strengthening behavior depends on the functional group incorporated into the reinforcing copolymer. The degree of strengthening was observed to follow the trend according to pendant functionality: phenol > primary benzamide > *N*-ethylbenzamide. The trend was attributed to the sensitivity of attractive hydrogen-bonding interactions to factors such as self-association and steric hindrance. In the case of the benzamide copolymers composition drift may also contribute to the observed strengthening effect. Clearly, a range of interfacial properties is now readily accessible through the appropriate choice of functionalized random copolymer.

Acknowledgment. Financial support of the Cornell Materials Science Center under a grant from the National Science Foundation (DMR 9632275) is gratefully acknowledged. We also appreciate the use of the Ion Beam Analysis Central Facility of the Materials Science Center and the invaluable assistance of P. Revesz and N. Szabo of this facility. Additional support from the National Science Foundation (DMR-9796106) is also acknowledged.

CM970432H

(23) Bandrup, J., Immergut, E. H., Eds. *Polymer Handbook*; John Wiley & Sons: New York, 1989.
(24) Vivas de Meftahi, M.; Fréchet, J. M. J. *Polymer*, **1988**, *29*, 477.